PERGAMON International Journal of Non-Linear Mechanics 34 (1999) 709–721

INTERNATIONAL JOURNAL OF NON-LINEAR MECHANICS

Asymptotic treatment of the trapeze effect in finite element cross-sectional analysis of composite beams

Bogdan Popescu, Dewey H. Hodges*

School of Aerospace Engineering, Georgia Institute of Technology, Atlanta, GA 30332-0150, USA

Received for publication 17 August 1998

Abstract

Early analyses for numerical cross-sectional analysis of anisotropic beams were based on linear elasticity theory. For more general treatment of non-linear phenomena, asymptotic formulations can serve as the basis for the numerical method, say a finite element method. When based on geometrically non-linear elasticity theory, an intermediate result of such analyses is frequently the splitting of the non-linear 3-D problem into a linear 2-D analysis of the cross section and a non-linear 1-D analysis along the beam. Thus, the published work to date cannot treat the so-called "trapeze effect", because it stems from non-linearity of the cross-sectional analysis. Herein, a non-linear numerical cross-sectional analysis is presented, based on the variational-asymptotic method and capable of treating cross sections of arbitrary geometry and generally anisotropic material. This type of analysis is particularly important in rotating structures, such as helicopter rotor blades. Results from this model are compared with those available in the literature, both theoretical and experimental.

Keywords: Beams; Composite; Non-linear; Asymptotic; Warping; Cross-sectional analysis

1. Introduction

Beam-like structures are common in engineering practice, e.g., rotor blades, turbine blades, high-aspect-ratio wings, and girders can all be represented as beams. Structural analysis of such members is currently based on three-dimensional (3-D) solid modeling, plate/shell elements to model thin-walled structures, and beam finite elements. The first two of these approaches require significant modeling and computational effort and are frequently inappropriate, especially in preliminary design stages. On the other hand, beam finite elements are computationally efficient and are available in all commercial finite element codes. The use of beam finite elements, however, requires a set of cross-sectional elastic constants as input. For all but the most trivial configurations, these constants must be determined from a separate cross-sectional analysis. Presently available commercial finite element codes lack the capability of performing cross-sectional analysis for beams, and cross-sectional elastic constants for beams made of general anisotropic-material cannot be determined analytically except

* Corresponding author. Fax: +1 404 894 9313; e-mail: dewey.hodges@ae.gatech.edu

0020-7462/99/$ – see front matter
PII: S0020-7462(98)00049-3

in the case of very specialized cross-sectional geometry. The present paper provides an increase in capability for a recently developed cross-sectional analysis. Such an approach is able to deliver fast and compact results which can then be used in a much more efficient 1-D formulation.

The loads peculiar to rotating beams are responsible for centrifugal and Coriolis forces and call for rigorous treatment of various couplings and non-linear effects that may occur. In this context, the so-called "trapeze effect" is a non-linear effect due to extension-torsion coupling in beams undergoing large axial forces. This effect has been found to be important in applications involving helicopter rotor blades, propellers and turbomachinery blades which, in all cases, have to cope with large centrifugal forces.

With the advent of composite rotor blades, values for the additional (coupling) stiffness constants need to be accurately determined. Published analyses can be found for numerical cross-sectional analysis of anisotropic beams (see [1, 2] and the references cited therein). Although most of the earlier works are based on linear elasticity theory, the resulting cross-sectional constants have been frequently used in geometrically non-linear analyses. One should not expect this sort of an ad hoc approach to be sufficient for general treatment of non-linear phenomena.

In recent years, to remedy this problem, asymptotic formulations have been developed which serve as the basis for a numerical method, say a finite element method [2]. Starting with geometrically non-linear elasticity theory, one finds frequently that a helpful intermediate result is a splitting of the non-linear problem into a linear 2-D analysis and a non-linear 1-D analysis. However, published work in this area to date cannot yet treat the so-called "trapeze effect", because it stems from non-linearity of the cross-sectional analysis.

For composite beams the trapeze effect has been treated by means of a simple expression, attributed to Rehfield in [3]. Also there is the finite element approach of [4], intended to augment [5]. Recently, an analytical asymptotic solution for anisotropic strips was presented in [6, 7]. To our knowledge, however, there are no analyses within an asymptotic framework which capture the trapeze effect in generally anisotropic beams of arbitrary cross-sectional geometry. The present work is intended to fill this gap and allow for an asymptotically correct determination of the class of those effects which render the cross-sectional analysis non-linear for beams of arbitrary cross-sectional geometry and made of generally anisotropic materials. This is accomplished by using a finite element discretization of the cross section. The measure for "correctness" is provided by the variational-asymptotic method. This gets rid of the ad hoc assumptions which are frequently invoked in the process of specializing the exact 3-D elasticity to beams regarded as 1-D structures.

As far as the "trapeze" effect is generally concerned, one can talk basically about two different aspects of it. One is the change in torsional stiffness due to an axial load, and other is the untwisting of pretwisted beams of non-circular cross section due to an axial load [8]. The former is due to the presence of certain non-linear terms in the strain field due to moderate local rotation [9]. The latter is mostly due to geometrical considerations and has been treated in [8] for isotropic beams and in [10] for generally anisotropic beams.

As a prime consequence of the above effects, both the aerodynamics and the torsional vibration characteristics will be affected, which in turn will modify the aeroelastic stability boundary. Such analyses are available in Refs. [3, 11]. The effect is also inevitable when dealing with axial-torsional buckling of columns with open sections, where a compressive axial force is applied as opposed to a extensional force in the case of rotating blades.

2. Previous work

The first recorded observation of the "trapeze" effect came with experiments conducted by Campbell [12] and was investigated by Pealing [13]. The first explanation came from Buckley [14], who first considered the beam as being composed "of a number of consecutive fibers, parallel to the length of the strip." Differences in material anisotropic properties for different specimens were correctly ascribed to experimental discrepancies. It was stated in his work that the "bifilar effect" (the term for "trapeze effect" at the time of the paper) is

independent of the fibrous structure of the material of the strip, whereas the torsional rigidity strongly depends on it. It is also known that both depend on the cross-sectional geometry but in complementary directions: when one increases the other decreases.

In his work, Wagner [15] also uses the hypothesis of longitudinal material fibers, but he primarily treats increases in the torsional rigidity due to restrained torsion of thin-walled open section configurations, the so-called "Vlasov effect". He also considers the trapeze term in his equations for torsional buckling, but the derivation is similar to Buckley's, as also observed by Goodier [16]. The hypothesis of longitudinal fibers is based on intuitive arguments, and counter examples have been noted [8]. In the absence of more powerful analyses, the domain of validity cannot be determined. There is also the need to consider the possible redistribution of stresses on the cross section due to non-linearities.

Another approach was offered by Biot [17]. He uses second-order rotation effects in conjunction with a state of prestress of the beam in order to capture the trapeze term. Biot's analysis also pointed out that the effect is significant for "sections having a low torsional rigidity in their natural state". Goodier's approach [16] is similar to Biot's method but considers Trefftz's stress components and also attempts to determine the influence of bending on torsional rigidity.

Houbolt and Brooks [18] developed equations of motion for rotating beams which included the trapeze stiffening and pretwist terms. They implicitly used Buckley's hypothesis, which allows for a correct determination of the increase in torsional rigidity but turns out to give incomplete results when used for the determination of the pretwist effect as pointed out by Hodges [8] and Rosen [19]. Both of these references consider the role of curvilinear coordinates, and the former along with [20] treat the problem with a non-linear definition of the strain, both of which are necessary ingredients toward a consistent treatment of the problem.

Trapeze effects were considered in specialized helicopter blade dynamics analyses (see [3, 21, 22]) and in turbomachinery applications (see [23, 24]). As a general trend, it seems that Buckley's hypothesis is quite popular in spite of the controversy that has surrounded it. Nevertheless, the method has been improved (see [25] for an analysis) over the years but a certain degree of arbitrariness still remains.

It is with this in mind that the present analysis was developed. So, a non-linear, numerical cross-sectional analysis is developed herein in an asymptotic fashion to treat cross sections of arbitrary geometry and made of generally anisotropic materials. As seen from the literature survey, this type of analysis is particularly important in rotating structures, such as helicopter rotor blades. Results from this model will be compared with those available in the literature, both theoretical and experimental.

3. Beam kinematics

We consider an initially straight and untwisted beam undergoing extension, torsion, and bending in two directions. Initial curvature and twist, shear deformation and restrained warping effects need not be considered here in light of the following reasoning: introducing h as a characteristic dimension of the cross section, ℓ as the characteristic wavelength of deformation along the beam, R as the maximum radius of curvature/twist, and ε as the maximum strain in the beam, one can characterize the strain energy of an elastic beam as an asymptotic series. The leading terms of this series contain the so-called classical theory, which is a quadratic form in terms of extension, twist, and bending generalized strain measures [26, 2]. All other terms in the series are multiplied by some small paramter(s). Initial curvature and twist are refinements of the order of h/R, $(h/R)^2$, etc., treated in [10], for example. Non-classical effects such as transverse shear and the Vlasov effect are refinements with respect to the leading terms of the order of $(h/\ell)^2$, which will be presented in later papers. The trapeze effect can be considered as a subset of the terms present in the correction that is $O(\varepsilon)$ relative to the leading terms.[1] It is fortunate indeed

[1] It should be noted that the terms of interest are formally $O(\varepsilon)$ relative to the leading terms, but a portion of these terms have numerically large coefficients for some cross-sectional configurations.

that other small parameters can be ignored in the calculation of the $O(\varepsilon)$ refinement, because it would be practically impossible to consider still higher-order refinements, such as those of order $\varepsilon h/R$ for example.

3.1. Beam in the undeformed state

In order to carry out this development, we orient the beam along the x_1-axis of a Cartesian system x_i, $i = 1, 2, 3$. Here and throughout the paper, Latin indices take values 1, 2, and 3, while Greek indices take values 2 and 3; repeated indices are summed over their ranges. The x_1-axis passes through the area centroids of each normal cross-sectional plane. Consider x_α to be the coordinates parallel to the cross-sectional plane. Finally, let the corresponding orthogonal unit vectors $\hat{\mathbf{b}}_i$ be along x_i.

From the framework defined in [27], the undeformed state is described by the position vector of a particle belonging to the actual cross section. Thus, we can write

$$\bar{\mathbf{r}}(x_1, x_2, x_3) = x_i \hat{\mathbf{b}}_i. \tag{1}$$

The covariant and contravariant base vectors for the undeformed state are simply equal to $\hat{\mathbf{b}}_i$.

3.2. Beam in the deformed state

The position vector of a point in the deformed structure may be defined as

$$\bar{\mathbf{R}}(x_1, x_2, x_3) = \mathbf{R}(x_1) + x_\alpha \hat{\mathbf{B}}\alpha(x_1) + w_i(x_1, x_2, x_3)\, \hat{\mathbf{B}}_i(x_1), \tag{2}$$

where $\hat{\mathbf{B}}_i = C_{ij}^{Bb} \hat{\mathbf{b}}_j$ are the unit basis vectors for the cross section of the deformed beam, $\mathbf{R}(x_1)$ is the position vector to points on the reference line of the deformed beam, and $w_i(x_1, x_2, x_3)$ represents both inplane and out-of-plane warping components. The nature of the constraints imposed on the warping below dictate the nature of the deformed beam reference line and reference cross sections, i.e. the specific definitions of C_{ij}^{Bb} and $\mathbf{R}$. The choice of constraints is not unique; we will use integral constraints which cause the resulting 1-D strain energy functional to be simple. These constraints are chosen to be

$$\langle \bar{\mathbf{R}} \rangle = \langle 1 \rangle \mathbf{R}, \quad \mathbf{B}_\alpha \cdot \mathbf{R}' = 0,$$
$$\mathbf{B}_2 \cdot \langle \bar{\mathbf{R}} x_3 \rangle = \mathbf{B}_3 \cdot \langle \bar{\mathbf{R}} x_2 \rangle \tag{3}$$

with the notation

$$\langle \bullet \rangle = \int_s \bullet \sqrt{g}\, \mathrm{d}x_2\, \mathrm{d}x_3. \tag{4}$$

This means that the deformed beam reference line is the average position of the material points in the deformed beam which made up the reference cross-sectional plane of the undeformed beam. This also implies that the warping is constrained so that

$$\langle w_i \rangle = 0,$$
$$\langle x_2 w_3 - x_3 w_2 \rangle = 0. \tag{5}$$

It follows that

$$\mathbf{R}' = (1 + \gamma)\, \hat{\mathbf{B}}_1, \tag{6}$$

where γ is the 1-D extensional strain measure of the beam. The other 1-D strain measures are

$$\kappa = \{\kappa_1\ \kappa_2\ \kappa_3\}^{\mathrm{T}} \tag{7}$$

which are the elastic twist measure and the bending measures in the two directions, respectively. The curvature vector is defined so that $\hat{\mathbf{B}}_i' = \kappa_j \hat{\mathbf{B}}_j \times \hat{\mathbf{B}}_i$. This will facilitate the writing of the covariant basis vectors in the deformed state, which are given by

$$\mathbf{G}_1 = \mathbf{R}' + x_\alpha \hat{\mathbf{B}}_\alpha' + w_i \hat{\mathbf{B}}_i' + \underline{w_i' \hat{\mathbf{B}}_i},$$
$$\mathbf{G}_2 = \hat{\mathbf{B}}_2 + w_{i,2} \hat{\mathbf{B}}_i,$$
$$\mathbf{G}_3 = \hat{\mathbf{B}}_3 + w_{i,3} \hat{\mathbf{B}}_i. \tag{8}$$

The underlined term contributes $O(h/\ell)$ terms relative to the leading terms of the 1-D energy, so we need not consider it here.

4. Green strain formulation

The deformation gradient can be expressed using the covariant base vectors of the deformed beam and the contravariant base vectors of the undeformed beam

$$\mathbf{A} = \mathbf{G}_i \hat{\mathbf{b}}_i. \tag{9}$$

For non-linear analysis the Green strain tensor is given by (see [28])

$$\mathbf{\Gamma} = \tfrac{1}{2}(\mathbf{A}^{\mathrm{T}} \cdot \mathbf{A} - \mathbf{I}). \tag{10}$$

As pointed out above, the leading terms in the strain energy constitute the classical theory of prismatic beams. The terms being derived here can be regarded as an $O(\varepsilon)$ refinement of the leading terms of the order of the strain. In light of the definition of the maximum strain book-keeping parameter

$$\varepsilon = \max(\gamma, h\kappa_1, h\kappa_2, h\kappa_3) \tag{11}$$

the expression for the matrix of 3-D strain components must contain all terms up through $O(\varepsilon^2)$, viz.,

$$\Gamma = (\Gamma_\varepsilon \varepsilon + \Gamma_h w) + (\underline{\Pi_{\varepsilon\varepsilon}\, \varepsilon_{nl}} + \underline{\Pi_{\varepsilon w}\, w} + \underline{\Pi_{ww}\, w}), \tag{12}$$

where the underlined terms are $O(\varepsilon^2)$. Note that $\Gamma = \lfloor\ \Gamma_{11}/2\Gamma_{12}/2\Gamma_{13}|\Gamma_{22}|2\Gamma_{23}|\Gamma_{33}\ \rfloor^{\mathrm{T}}$. The operators are given by

$$\Gamma_\varepsilon = \begin{bmatrix} 1 & 0 & x_3 & -x_2 \\ 0 & -x_3 & 0 & 0 \\ 0 & x_2 & 0 & 0 \\ 0 & 0 & 0 & 0 \\ 0 & 0 & 0 & 0 \\ 0 & 0 & 0 & 0 \end{bmatrix}, \tag{13}$$

$$\Gamma_h = \begin{bmatrix} 0 & 0 & 0 \\ \partial_2 & 0 & 0 \\ \partial_3 & 0 & 0 \\ 0 & \partial_2 & 0 \\ 0 & \partial_3 & \partial_2 \\ 0 & 0 & \partial_3 \end{bmatrix}, \tag{14}$$

$$\Pi_{\varepsilon\varepsilon} = \begin{bmatrix} \frac{1}{2} & \frac{x_2^2 + x_3^2}{2} & \frac{x_3^2}{2} & \frac{x_2^2}{2} & x_3 & -x_2 & -x_2\, x_3 \\ & & 0_{5\times 7} & & & & \end{bmatrix}, \tag{15}$$

$$\Pi_{\varepsilon w} = \begin{bmatrix} 0 & -\kappa_3 & \kappa_2 \\ \gamma^*\partial_2 + \kappa_3 & x_3\kappa_1\partial_2 & x_2\kappa_1\partial_2 - \kappa_1 \\ \gamma^*\partial_3 - \kappa_2 & x_3\kappa_1\partial_3 + \kappa_1 & x_2\kappa_1\partial_3 \\ & 0_{3\times 3} & \end{bmatrix}, \tag{16}$$

where $\gamma^* = \gamma - \kappa_3\, x_2 + \kappa_2\, x_3$ and

$$\Pi_{ww} = \begin{bmatrix} & 0_{3\times 3} & \\ \frac{1}{2}w_{1,2}\partial_2 & \frac{1}{2}w_{2,2}\partial_2 & \frac{1}{2}w_{3,2}\partial_2 \\ w_{1,2}\partial_3 & w_{2,2}\partial_3 & w_{3,2}\partial_3 \\ \frac{1}{2}w_{1,3}\partial_3 & \frac{1}{2}w_{2,3}\partial_3 & \frac{1}{2}w_{3,3}\partial_3 \end{bmatrix}. \tag{17}$$

The subscript α following the comma in $w_{i,\alpha}$ represents the partial derivative taken with respect to x_α, and $\partial_\alpha = \partial/\partial x_\alpha$. Finally, the column matrices for 1-D strains, the non-linear 1-D strains, and the warping are given by

$$\varepsilon = \lfloor\ \gamma\kappa_1\kappa_2\kappa_3\ \rfloor^{\mathrm{T}}, \tag{18}$$

$$\varepsilon_{nl} = \lfloor\ \gamma^2\kappa_1^2\kappa_2^2\kappa_3^2\gamma\kappa_2\gamma\kappa_3\kappa_2\,\kappa_3\ \rfloor^{\mathrm{T}}, \tag{19}$$

$$w = \lfloor\ w_1 w_2 w_3\ \rfloor^{\mathrm{T}}. \tag{20}$$

5. Finite element formulation

Considering a finite element formulation for the warping field one can write

$$w = [S]\, V, \tag{21}$$

where $[S]$ is the matrix of shape functions and V is the column matrix of nodal values of the warping. In order to obtain the strain energy per unit length of the beam, one has to integrate the strain energy density over the cross-sectional area. The strain energy density is given by

$$U = \tfrac{1}{2}\langle \Gamma^{\mathrm{T}} D \Gamma \rangle, \tag{22}$$

where D is the 6×6 symmetric material matrix. Since we are interested in only the $O(\varepsilon)$ refinement relative to the leading terms, one needs to retain terms only up to $O(\varepsilon^3)$ in the strain energy. This yields

$$\begin{aligned} 2U = {} & \varepsilon^{\mathrm{T}} D_{\varepsilon\varepsilon}\varepsilon + 2V^{\mathrm{T}} D_{h\varepsilon}\varepsilon + V^{\mathrm{T}} E V + 2\,\underline{\varepsilon_{nl}^{\mathrm{T}} S_{\varepsilon\varepsilon\varepsilon}\,\varepsilon} \\ & + 2\,\underline{V^{\mathrm{T}} S_{w\varepsilon\varepsilon}\,\varepsilon} + 2\,\underline{V^{\mathrm{T}} S_{ww\varepsilon}\,\varepsilon} + 2\,\underline{\varepsilon_{nl}^{\mathrm{T}} S_{\varepsilon\varepsilon h}\, V} \\ & + 2\,\underline{V^{\mathrm{T}} S_{w\varepsilon h}\, V} + 2\,\underline{V^{\mathrm{T}} S_{wwh}\, V}, \end{aligned} \tag{23}$$

where V is the column matrix that contains all the nodal values of the warping and expressions for the

material matrices are given in the appendix, Eqs. (A.1). The $O(\varepsilon^3)$ terms in the strain energy are underlined. The first approximation for the warping is obtained by considering the principal part of the strain energy (i.e. only second-order terms). The first-order warping field is the solution of

$$D_{h\varepsilon}\varepsilon + E\,V = H\psi_{\mathrm{c1}}\,\mu \tag{24}$$

where the column matrix μ contains the Lagrange multipliers which impose the constraints on warping. They are given by

$$\mu = \psi_{\mathrm{c1}}^{\mathrm{T}}\,D_{h\varepsilon}\,\varepsilon, \tag{25}$$

where ψ_{c1} forms the null-space of matrix E so that

$$E\psi_{\mathrm{c1}} = 0 \tag{26}$$

and H is a matrix defined as

$$H \triangleq \langle [S]^{\mathrm{T}}\,[S]\rangle. \tag{27}$$

Due to the indeterminacy introduced by the warping field, the matrix E is singular. The indeterminancy is removed by considering constraints in the warping field. To solve the system given by Eq. (24) the matrix E_{c1}^{+} must be introduced such that

$$EE_{\mathrm{c1}}^{+} = I - H\psi_{\mathrm{c1}}\,\psi_{\mathrm{c1}}^{\mathrm{T}}, \tag{28}$$

where ψ_{c1} contains the four columns corresponding to the vectors that span the null space of E.

6. Asymptotic approach

Suppose now that the warping for the non-linear problem is given by

$$w = \underbrace{w_0}_{h\varepsilon} + \underbrace{w_1}_{h\varepsilon^2}, \tag{29}$$

where w_1 is the perturbation of the warping field of order ε^2, and w_0 represents the solution of Eq. (24) and is therefore $O(\varepsilon)$. We require that the entire warping satisfies the same constraints (5). Since the initial warping already satisfies these constraints, it follows that the warping perturbation must satisfy them as well. Consider the finite element discretization

$$w = [S]\;V_0 + [S]\;V_1. \tag{30}$$

This determines that only $O(\varepsilon^2)$ terms need to be kept in the strain expression so that

$$\Gamma = \Gamma_\varepsilon\,\varepsilon + \Gamma_h\,V_0 + \underline{\Gamma_w\,V_1} + \underline{\Pi_{\varepsilon\varepsilon}\,\varepsilon_{\mathrm{n1}}} + \underline{\Pi_{\varepsilon w}\,V_0} + \underline{\Pi_{w_0 w}\,V_0} + O(\varepsilon^3), \tag{31}$$

where $\Pi_{w_0 w}$ is the Π_{ww} operator in Eq. (17) with only the first component of the warping. The underlined terms are $O(\varepsilon^2)$. Now let us substitute this expression into the energy, keeping only terms up to $O(\varepsilon^3)$. The strain energy becomes

$$\begin{aligned} 2U = {} & \varepsilon^{\mathrm{T}}\,D_{\varepsilon\varepsilon}\,\varepsilon + 2\,V_0^{\mathrm{T}}\,D_{h\varepsilon}\,\varepsilon + V_0^{\mathrm{T}}\,E\,V_0 + 2\,V_1^{\mathrm{T}}\,D_{h\varepsilon}\,\varepsilon \\ & + 2\,\underline{\varepsilon_{nl}^{\mathrm{T}}\,S_{\varepsilon\varepsilon\varepsilon}\,\varepsilon} + 2\,\underline{V_0^{\mathrm{T}}\,S_{w\varepsilon\varepsilon}\,\varepsilon} + \underline{2\,V_0^{\mathrm{T}}\,S_{ww_0\varepsilon}\,\varepsilon} \\ & + 3\,V_1^{\mathrm{T}}\,E\,V_0 + 2\,\underline{\varepsilon_{\mathrm{n1}}^{\mathrm{T}}\,S_{\varepsilon\varepsilon h}\,V_0} + 2\,\underline{V_0^{\mathrm{T}}\,S_{w\varepsilon h}\,V_0} \\ & + 2\,\underline{V_0^{\mathrm{T}}\,S_{ww_0 h}\,V_0} \end{aligned} \tag{32}$$

where the underlined terms are $O(\varepsilon^3)$ and

$$\begin{aligned} S_{w_0 w\varepsilon} &= \langle [\Pi_{w_0 w}\,S]^{\mathrm{T}}\;D\,\Gamma_\varepsilon\rangle, \\ S_{w_0 wh} &= \langle [\Pi_{w_0 w}\,S]^{\mathrm{T}}\;D\,[\Gamma_h\,S]\rangle. \end{aligned} \tag{33}$$

According to the results from the variational-asymptotic method (see [29, 30]), the part of the strain energy containing the perturbation terms must vanish. This means we get the equation

$$V_1^{\mathrm{T}}\,D_{h\varepsilon}\,\varepsilon + V_1^{\mathrm{T}}\,EV_0 = 0. \tag{34}$$

According to the warping constraint equation, $V_1^{\mathrm{T}}H\psi_{\mathrm{c1}} = 0$. Thus, using Eq. (24) this equation is identically satisfied.

This result is crucial because it proves the remarkable result that only the first (i.e. the classical) approximation for the warping is sufficient in order to deliver the 1-D strain energy asymptotically correct up to the third order in strain. However, it is noteworthy to remark that this proof does not imply the calculated warping is exact since we miss the contribution of V_1. Theoretically, it can be calculated, but practically it requires a tremendous effort and provides little added benefit. One has to do so only if higher-order corrections to the displacement, strain and/or stress fields are needed.

7. Mathematical realization

In order to carry out further calculations to actually determine the constitutive relation for the

cross section, it is necessary to somehow pull out the unknown 1-D strain from inside the matrices where they are buried (i.e. $\Pi_{\varepsilon w}$ and Π_{ww}) and the 1-D strain measures contained in the warping.

The first approximation of the warping is written for an element

$$w_0 = S\hat{V}_0\,\varepsilon, \tag{35}$$

where S is the matrix of the shape functions, and $\hat{V}$ is determined by the solution of Eq. (24). For simplicity of notation the index "0" will be dropped. The ith component of the warping can be written using the summation rule over repeated indices as

$$\begin{aligned} w_i &= \gamma S_{ij}\hat{V}_{j1} + \kappa_1 S_{ij}\hat{V}_{j2} + \kappa_2 S_{ij}\hat{V}_{j3} + \kappa_3 S_{ij}\hat{V}_{j4} \\ &= \varepsilon_k S_{ij}\hat{V}_{jk} \end{aligned} \tag{36}$$

which helps us to write the strain components, which are non-linear functions of the 1-D strain measures, in a more convenient form.

One can express the components of the 3-D strain due to part $\Pi_{\varepsilon w}$ as

$$\Gamma_{\varepsilon w} = (\gamma\,\Gamma_{\varepsilon w}^{(\gamma)} + \kappa_1\Gamma_{\varepsilon w}^{(\kappa_1)} + \kappa_2\,\Gamma_{\varepsilon w}^{(\kappa_2)} + \kappa_3\Gamma_{\varepsilon w}^{(\kappa_3)})\,\varepsilon, \tag{37}$$

where

$$\Gamma_{\varepsilon w}^{(\gamma)} = \begin{bmatrix} 0 \\ S_{1j,2}\,\hat{V}_{j-} \\ S_{1j,3}\,\hat{V}_{j-} \\ 0_{-3} \end{bmatrix}, \tag{38}$$

$$\Gamma_{\varepsilon w}^{(\kappa_1)} = \begin{bmatrix} 0 \\ (x_3 S_{2j,2} + x_2 S_{3j,2} - S_{3j})\,\hat{V}_{j-} \\ (x_3 S_{2j,3} + x_2 S_{3j,3} + S_{2j})\hat{V}_{j-} \\ 0_{-3} \end{bmatrix}, \tag{39}$$

$$\Gamma_{\varepsilon w}^{(\kappa_2)} = \begin{bmatrix} S_{3j}\,\hat{V}_{j-} \\ x_3\,S_{1j,2}\hat{V}_{j-} \\ (x_3\,S_{1j,3} - S_{1j})\,\hat{V}_{j-} \\ 0_{-3} \end{bmatrix}, \tag{40}$$

$$\Gamma_{\varepsilon w}^{(\kappa_3)} = \begin{bmatrix} -\,S_{2j}\,\hat{V}_{j-} \\ (-\,x_2\,S_{1j,2} + S_{1j})\,\hat{V}_{j-} \\ -\,x_2\,S_{1j,3}\,\hat{V}_{j-} \\ 0_{-3} \end{bmatrix}, \tag{41}$$

and where the notation $\hat{V}_{j-}$ means the jth row of matrix $\hat{V}$.

The components of the 3-D strain due to part Π_{ww} can be cast in the same form, so that

$$\Gamma_{ww} = (\gamma\Gamma_{ww}^{(1)} + \kappa_1\Gamma_{ww}^{(2)} + \kappa_2\Gamma_{ww}^{(3)} + \kappa_3\Gamma_{ww}^{(4)})\,\varepsilon, \tag{42}$$

where

$$\Gamma_{ww}^{(k)} = \begin{bmatrix} 0_{-3} \\ \frac{1}{2}S_{pj,2}\,S_{pl,2}\,\hat{V}_{jk}\,\hat{V}_{l-} \\ S_{pj,2}\,S_{pl,3}\,\hat{V}_{jk}\,\hat{V}_{l-} \\ \frac{1}{2}S_{pj,3}\,S_{pl,3}\,\hat{V}_{jk}\hat{V}_{l-} \end{bmatrix}, \tag{43}$$

Finally, the $\Pi_{\varepsilon\varepsilon}$ part of the strain can take a similar form (but not unique) if we consider

$$\Gamma_{\varepsilon\varepsilon}^{(\gamma)} = \begin{bmatrix} \frac{1}{2} & 0 & x_3 & 0 \\ & 0_{5\times 4} & & \end{bmatrix}, \tag{44}$$

$$\Gamma_{\varepsilon\varepsilon}^{(\kappa_1)} = \begin{bmatrix} 0 & \frac{1}{2}(x_2^2 + x_3^2) & 0 & 0 \\ & 0_{5\times 4} & & \end{bmatrix}, \tag{45}$$

$$\Gamma_{\varepsilon\varepsilon}^{(\kappa_2)} = \begin{bmatrix} 0 & 0 & \frac{1}{2}x_3^2 & -\,x_2\,x_3 \\ & 0_{5\times 4} & & \end{bmatrix}, \tag{46}$$

$$\Gamma_{\varepsilon\varepsilon}^{(\kappa_3)} = \begin{bmatrix} -\,x_2 & 0 & 0 & \frac{1}{2}x_2^2 \\ & 0_{5\times 4} & & \end{bmatrix}. \tag{47}$$

Hence,

$$\Gamma_{\varepsilon\varepsilon} = (\gamma\Gamma_{\varepsilon\varepsilon}^{(\gamma)} + \kappa_1\Gamma_{\varepsilon\varepsilon}^{(\kappa_1)} + \kappa_2\Gamma_{\varepsilon\varepsilon}^{(\kappa_2)} + \kappa_3\Gamma_{\varepsilon\varepsilon}^{(\kappa_3)})\,\varepsilon. \tag{48}$$

Considering the symbols ε_k and k equivalent and interchangeable, then

$$\Gamma_k = \Gamma_{\varepsilon\varepsilon}^{(k)} + \Gamma_{\varepsilon w}^{(k)} + \Gamma_{ww}^{(k)} \tag{49}$$

which enables us to write the strain over the ith element as

$$\Gamma^{(i)} = (\Gamma_{\mathrm{cl}} + \gamma\Gamma_{\gamma} + \kappa_1\Gamma_{\kappa_1} + \kappa_2\Gamma_{\kappa_2} + \kappa_3\Gamma_{\kappa_3})\,\varepsilon, \tag{50}$$

where Γ_{cl} is the classical strain field.

The strain energy is then found by integrating over all elements and can be cast in a form involving four more non-classical stiffness matrices

$$U = \varepsilon^{\mathrm{T}}(\tfrac{1}{2}\,A_{\mathrm{cl}} + \gamma\mathrm{A}_{\gamma} + \kappa_1 B_{\kappa_1} + \kappa_2 C_{\kappa_2} + \kappa_3 D_{\kappa_3})\,\varepsilon, \tag{51}$$

where A_{cl} is the classical stiffness matrix.

The cross-sectional stiffness matrix is obtained by expressing the resultant forces on the beam cross section as

$$R \triangleq \begin{Bmatrix} F_1 \\ M_1 \\ M_2 \\ M_3 \end{Bmatrix} = \begin{Bmatrix} \dfrac{\partial U}{\partial \gamma} \\ \dfrac{\partial U}{\partial \kappa_1} \\ \dfrac{\partial U}{\partial \kappa_2} \\ \dfrac{\partial U}{\partial \kappa_3} \end{Bmatrix}. \tag{52}$$

8. Applications

8.1. Isotropic beams

The classical test case is given by a beam made of isotropic material, which is expected to give the basic idea about the impact of the non-linearities. For the isotropic case the matrices are obtained in the form presented in the appendix, Eqs. (A.2)–(A.6). Hence, according to Eq. (52) the non-linear loads are obtained as follows:

$$F_1 = \gamma EA + 2\kappa_1^2 B_{12} + 2\kappa_2^2 (A_{33} + C_{13}) + 2\kappa_2^3 D_{14}, \tag{53}$$

$$M_1 = \kappa_1 (GJ + \underline{\underline{4 B_{12} \gamma}}), \tag{54}$$

$$M_2 = \kappa_2 [EI_2 + \underline{4(A_{33} + C_{13})\gamma}], \tag{55}$$

$$M_3 = \kappa_3 (EI_3 + \underline{4 D_{14} \gamma}). \tag{56}$$

The doubly underlined term represents the increase in torsional rigidity due to axial tensile load. The singly underlined terms are similar terms representing the increase in bending stiffness due to the axial load. These last terms are usually small and are neglected, but it not possible to say that they never turn out to be important. The only place in the literature where we found a derivation containing terms of this type is [16].

8.2. Composite beams

Another illustrative case is provided by Winckler's system (see [31]) consisting of an antisymmetric composite strip with extension-twist coupling. The resulting linear and non-linear stiffness matrices are given in the appendix, Eqs. (A.7)–(A.11). For this case the relations for the resultant interior forces will have more non-linear contributions:

$$F_1 = \gamma [A_{\mathrm{cl}_{11}} + \underline{\kappa_1 (4A_{12} + 2B_{11}) + 3\gamma A_{11}}] + 2\kappa_1 A_{\mathrm{cl}_{12}} + \kappa_1^2 (2B_{12} + A_{22}) + \kappa_2^2 (2C_{13} + A_{33}) + \kappa_3^2 (2D_{14} + A_{44}), \tag{57}$$

$$M_1 = \kappa_1 [A_{\mathrm{cl}_{22}} + \underline{\underline{\gamma (4B_{12} + 2A_{22}) + 3\kappa_1 B_{22}}}] + 2_{\mathrm{cl}_{12}} + \gamma^2 (2A_{12} + B_{11}) + \kappa_2^2 (2C_{23} + B_{33}) + \kappa_3^2 (2D_{24} + B_{44}), \tag{58}$$

$$M_2 = \kappa_2 A_{\mathrm{cl}_{33}} + \underline{\gamma \kappa_2 (2A_{33} + 4C_{13}) + \kappa_1 \kappa_2 (2B_{33} + 4C_{23})}, \tag{59}$$

$$M_3 = \kappa_3 A_{\mathrm{cl}_{44}} + \underline{\gamma \kappa_3 (2A_{44} + 4D_{14}) + \kappa_1 \kappa_3 (2B_{44} + 4D_{24})}. \tag{60}$$

The underlined terms are non-linear contributions to the linear stiffnesses, and the doubly underlined term is the main effect which gives the increase in torsional rigidity.

8.3. A "rotor blade" problem

One case of interest is given by an axially loaded beam free to twist and bend which represents a typical rotating blade configuration in vacuum

$$F_1 \neq 0; \quad M_1 = 0; \quad M_2 = 0; \quad M_3 = 0. \tag{61}$$

Eq. (51) is accurate, but for existing 1-D codes some extensive reprogramming may be needed since it involves non-linear terms in the 1-D strain measures. A somewhat more desirable expression for finding the column matrix of interior forces R to accomodate existing analyses would be

$$R = A\varepsilon \tag{62}$$

which preserves the form of the classical expression but where the elements of the stiffness matrix A

may be functions of the interior forces, in particular for our case, the stretching force F_1. This is motivated by the fact that for rotating beams, this force is known a priori as the centrifugal force. This is the idea in Rehfield's model (see [3]), which alters the torsional rigidity term by adding a contribution proportional with the applied stretching force

$$A_{22} = A_{\mathrm{cl}_{22}} + \left(\frac{A_{\mathrm{cl}_{33}} + A_{\mathrm{cl}_{44}}}{A_{\mathrm{cl}_{11}}}\right)\bar{F}_1, \tag{63}$$

where $\bar{F}_1$ is the equilibrium value of the axial force.

To obtain the coresponding increase in torsional rigidity requires a separate analysis in which the general relations, Eqs. (51) and (52), are transformed in order to accomodate Eq. (61). This is best done using symbolic computation, where advantage should be taken of neglecting certain small terms which appear due to the structure of the non-linear contributions. This process yields results which are specific to each application, and it seems that no general expression can be given a priori.

8.4. Numerical results

The theoretical development described above has been implemented in the existing code VABS (variational-asymptotic beam section); see [2]. The code can handle arbitrary cross-sectional geometries of initially curved and twisted composite beams [10].

A well-documented test case is provided with both experimental and theoretical results by Armanios *et al.* [32]. They considered two specimens with the same material properties, given in Table 1 and a pretwist of -5°. The layup for specimen 1 is $[20_2/-70_4/20_2/-20_2/70_4/-20_2]_T$ while for specimen 2 it is $[30_2/-60_4/30_2/-30_2/60_4/-30_2]_T$.

For the case of the first specimen the resultant interior forces are determined according to Eq. (52). These results are presented together with the experimental results of [32] in Figs. 1 and 2, where the tip twist angle θ was represented as a function of the axial force F. A mesh of 160, six-node isoparametric finite elements was used. The results show excellent agreement with experiment, and the present results are right on top of those from [6].

Table 1
Geometrical and material characteristics for the extension-twist coupling experiments

$L = 254$ mm
$2b = 25.4$ mm
$h = 1.168$ mm
$E_{11} = 135.6$ GPa
$E_{22} = E_{33} = 9.9$ GPa
$G_{12} = G_{13} = 4.2$ GPa
$G_{23} = 2.3$ GPa
$v_{12} = v_{13} = 0.3$
$v_{23} = 0.5$

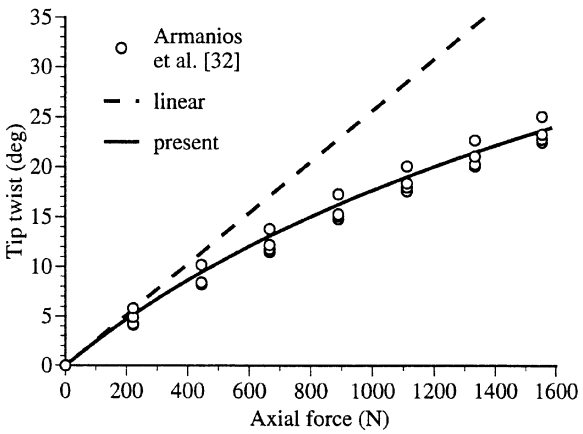

Fig. 1. Extension–twist coupling in specimen 1.

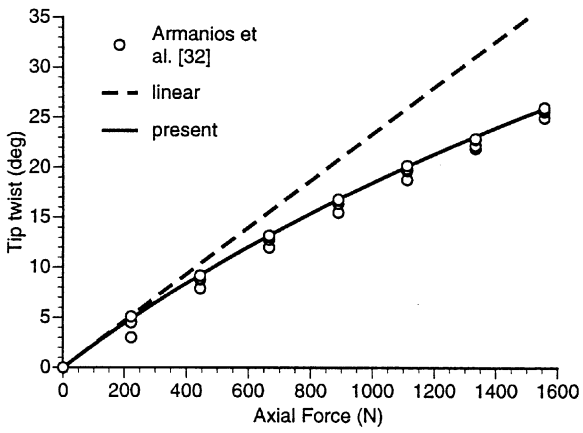

Fig. 2. Extension–twist coupling in specimen 2.

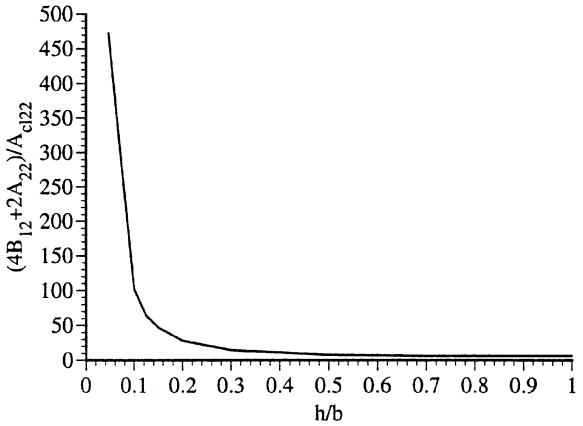

Fig. 3. Trapeze effect variation with the aspect ratio.

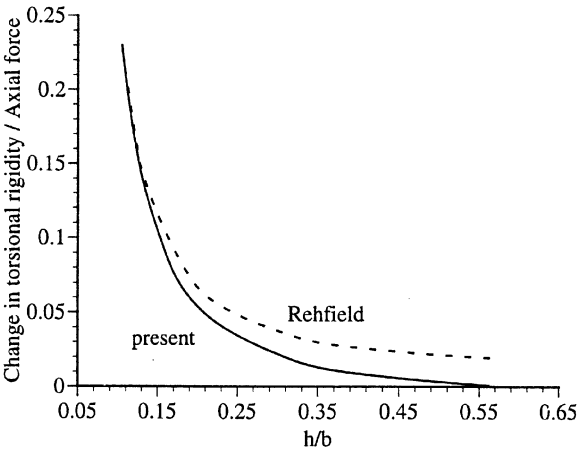

Fig. 4. Trapeze effect variation with the aspect ratio (boxbeam).

As the cross section departs from a strip configuration, the trapeze effect becomes less and less important compared to the overall torsional rigidity. For the layup given by specimen 1 above, the thickness of the strip was gradually increased while the area was kept constant. The parameter

$$\frac{\partial^2 M_1/\partial\gamma\partial\kappa_1}{\partial M_1/\partial\kappa_1|_{\kappa_1=0,\gamma=0}} = \frac{4B_{12}+2A_{22}}{A_{\mathrm{cl}_{22}}} \tag{64}$$

is taken as a measure of the contribution given by the trapeze effect. Its variation as the cross section gradually changes from a thin strip to a square configuration is represented in Fig. 3 as a function of the aspect ratio (h/b) of the cross section. It can be seen that for (h/b) larger than approximately 0.2 the effect rapidly becomes less significant. For example, taking a limit axial strain $\gamma_{11} = 0.01$, the trapeze effect will account of about 25% increase in torsional rigidity at $h/b = 0.2$ while for $h/b = 0.3$ the contribution is of about 15%. This is down from 100% at $h/b = 0.1$ or 500% at $h/b = 0.05$ where the torsional rigidity due to the trapeze effect is dominant.

For cases in which an axial force is involved (such as in the case of the centrifugal force in rotating blades), Rehfield's model provides an adequate way to easily accomodate the trapeze effect contribution without extensive modification of a linear cross-sectional analyses. For the two laminates presented above the results were indeed in very good agreement with the present results. To further test the validity of Rehfield's model a couple of other geometries departing from a strip-like configuration have been considered. As a closed cross section configuration, the "symmetric 4" bending-twist coupled box-beam of [33] was selected. The aspect ratio has been varied while the thickness and width were kept constant. For numerical values, the analysis is carried out considering an axial force corresponding to the limiting case of an axial strain of $\gamma = 0.01$. The absolute increase in torsional rigidity was found to differ by as much as 200% of the value predicted by Rehfield's formula. However, because the torsional rigidity is significantly larger for closed cross sections, the results indicate that Rehfield's formula overpredicts the total torsional rigidity by approximately 2% for higher aspect ratios. This is presented in Fig. 4. Finally, *I*-beams, a circular tube with a cutout and a semicircle have been considered as other examples of open cross sections. For all these the differences observed between Rehfield's formula and the present model were minimal.

9. Conclusions

The modeling capability of a recently developed cross-sectional analysis [2] was increased to include non-linear phenomena, such as the trapeze

effect. Based on the variational-asymptotic method it was possible to show that the first approximation of the warping, derived for the classical problem, is sufficient to render the strain energy correct up through the third order in the 1-D strain measures. For the problem of small strain and moderate local rotations this is sufficient.

The principal correction to the classical theory of the order of maximum strain, for the types of structures investigated, is the non-linear extension-twist coupling. This is especially the case when thin-walled open cross sections or strip-like configurations are involved. Since for these cases the torsional stiffness is relatively small, the trapeze terms may become dominant.

The results for the two strip-like configurations presented above were in very good agreement with both experimental and theoretical results in the literature. The finite element mesh is similar to that used for the classical problem and the increase in the computational effort is less than 6% primarily due to the fact that the warping field does not need to be recalculated. Also, the input data remains practically unchanged. This makes the implementation quite easy to use for practical problems of any complexity.

It should be noted that Rehfield's formula provides a way to estimate the change in torsional rigidity as a function of the applied axial force which is in general a known quantity. For open cross sections the formula gives an accurate estimation, within a 2% error margin relative to the overall stiffness value. For closed cross sections departing from a strip-like geometry, the formula performs poorly in assessing the trapeze effect, but this is not a serious problem because the torsional rigidity of the unloaded beam dominates the contribution from the trapeze effect. This shows that, for the case of a beam under axial force, Rehfield's model is a good substitute for torsionally soft beams with simple cross-sectional geometries. However, when precision is important or when one is in doubt about the actual values, as it may be the case for some arbitrary cross-sectional geometry, the use of the present method is recommended.

Finally, it is noted that, in addition to the trapeze terms, which couple extension and twist, the non-linear cross-sectional analysis gives rise to other non-linear coupling terms in the 1-D constitutive law. For all cases checked to date, these terms are negligibly small. However, it cannot be ruled out that these terms may turn out to be non-negligible in certain applications. To determine whether or not this is the case, additional research is required.

Appendix

Definitions of system matrices:

$$
\begin{aligned}
&D_{\varepsilon\varepsilon} = \langle \Gamma_\varepsilon^{\mathrm{T}} D \Gamma_\varepsilon \rangle,\\
&D_{h\varepsilon} = \langle [\Gamma_h S]^{\mathrm{T}} D \Gamma_\varepsilon \rangle,\\
&E = \langle [\Gamma_h S]^{\mathrm{T}} D [\Gamma_h S] \rangle,\\
&S_{\varepsilon\varepsilon\varepsilon} = \langle \Pi_{\varepsilon\varepsilon}^{\mathrm{T}} D \Gamma_\varepsilon \rangle,\\
&S_{\varepsilon\varepsilon h} = \langle \Pi_{\varepsilon\varepsilon}^{\mathrm{T}} D [\Gamma_h S] \rangle,\\
&S_{w\varepsilon\varepsilon} = \langle [\Pi_{\varepsilon w} S]^{\mathrm{T}} D \Gamma_\varepsilon \rangle,\\
&S_{w\varepsilon h} = \langle [\Pi_{\varepsilon w}^{\mathrm{T}} S]^{\mathrm{T}} D [\Gamma_h S] \rangle,\\
&S_{ww\varepsilon} = \langle [\Pi_{ww}^{\mathrm{T}} S]^{\mathrm{T}} D \Gamma_\varepsilon \rangle,\\
&S_{wwh} = \langle [\Pi_{ww}^{\mathrm{T}} S]^{\mathrm{T}} D [\Gamma_h S] \rangle.
\end{aligned} \tag{A.1}
$$

Stiffness matrices for the isotropic strip:

$$
A_{\mathrm{cl}} = \begin{bmatrix} EA & 0 & 0 & 0 \\ 0 & GJ & 0 & 0 \\ 0 & 0 & EI_2 & 0 \\ 0 & 0 & 0 & EI_3 \end{bmatrix}, \tag{A.2}
$$

$$
A_\gamma = \begin{bmatrix} 0 & 0 & 0 & 0 \\ 0 & 0 & 0 & 0 \\ 0 & 0 & 2A_{33} & 0 \\ 0 & 0 & 0 & 0 \end{bmatrix}, \tag{A.3}
$$

$$
B_{\kappa_1} = \begin{bmatrix} 0 & B_{12} & 0 & 0 \\ B_{12} & 0 & 0 & 0 \\ 0 & 0 & 0 & 0 \\ 0 & 0 & 0 & 0 \end{bmatrix}, \tag{A.4}
$$

$$C_{\kappa_2} = \begin{bmatrix} 0 & 0 & C_{13} & 0 \\ 0 & 0 & 0 & 0 \\ C_{13} & 0 & 0 & 0 \\ 0 & 0 & 0 & 0 \end{bmatrix}, \tag{A.5}$$

$$D_{\kappa_3} = \begin{bmatrix} 0 & 0 & 0 & D_{14} \\ 0 & 0 & 0 & 0 \\ 0 & 0 & 0 & 0 \\ D_{14} & 0 & 0 & 0 \end{bmatrix}. \tag{A.6}$$

Stiffness matrices for anisotropic strip:

$$A_{\mathrm{cl}} = \begin{bmatrix} A_{\mathrm{cl}_{11}} & A_{\mathrm{cl}_{12}} & 0 & 0 \\ A_{\mathrm{cl}_{12}} & A_{\mathrm{cl}_{22}} & 0 & 0 \\ 0 & 0 & A_{\mathrm{cl}_{33}} & 0 \\ 0 & 0 & 0 & A_{\mathrm{cl}_{44}} \end{bmatrix}, \tag{A.7}$$

$$A_{\gamma} = \begin{bmatrix} A_{11} & A_{12} & 0 & 0 \\ A_{12} & A_{22} & 0 & 0 \\ 0 & 0 & A_{33} & 0 \\ 0 & 0 & 0 & A_{44} \end{bmatrix}, \tag{A.8}$$

$$B_{\kappa_1} = \begin{bmatrix} B_{11} & B_{12} & 0 & 0 \\ B_{12} & B_{22} & 0 & 0 \\ 0 & 0 & B_{33} & 0 \\ 0 & 0 & 0 & B_{44} \end{bmatrix}, \tag{A.9}$$

$$C_{\kappa_2} = \begin{bmatrix} 0 & 0 & C_{13} & 0 \\ 0 & 0 & C_{23} & 0 \\ C_{13} & C_{23} & 0 & 0 \\ 0 & 0 & 0 & 0 \end{bmatrix}, \tag{A.10}$$

$$D_{\kappa_3} = \begin{bmatrix} 0 & 0 & 0 & D_{14} \\ 0 & 0 & 0 & D_{24} \\ 0 & 0 & 0 & 0 \\ D_{14} & D_{24} & 0 & 0 \end{bmatrix}. \tag{A.11}$$

Acknowledgements

This work was supported by the National Rotorcraft Technology Center at Ames Research Center through the Center of Excellence for Rotorcraft Technology at the Georgia Institute of Technology.

References

[1] D.H. Hodges, A review of composite rotor blade modeling, A.I.A.A. J. 28 (1990) 561.
[2] C.E.S. Cesnik, D.H. Hodges, VABS: a new concept for composite rotor blade cross-sectional modeling, J. Amer. Helicopter Soc. 42 (1997) 27.
[3] M.V. Fulton, D.H. Hodges, Aeroelastic stability of composite hingeless rotor blades in hover – Part I: theory, Math. Comput. Modelling, 18 (1993) 1.
[4] M. Borri, P. Mantegazza, Some contributions on structural and dynamic modeling of helicopter rotor blades, l'Aerotecnica Missili e Spazio, 64 (1985) 143.
[5] V. Giavotto, M. Borri, P. Mantegazza, G. Ghiringhelli, V. Carmaschi, G.C. Maffioli, F. Mussi, Anisotropic beam theory and applications, Comput. and Struct. 16 (1983) 403.
[6] D.H. Hodges, D. Harursampath, C.E.S. Cesnik, Nonlinear strain field effects in anisotropic strips, Proc. Recent Developments Solid Mech., Rio de Janeiro, Brazil, 1996, pp. 71–78.
[7] D.H. Hodges, D. Harursampath, C.E.S. Cesnik, Non-classical effects in nonlinear analysis of anisotropic strips, Int. J. Non-Linear Mech. (1998), to appear.
[8] D.H. Hodges, Torsion of pretwisted beams due to axial loading, *J. Appl. Mech.* 47 (1980) 393.
[9] D.A. Danielson, D.H. Hodges, A beam theory for large global rotation, moderate local rotation, and small strain, J. Appl. Mech. 55 (1988) 179.
[10] C.E.S. Cesnik, D.H. Hodges, V.G. Sutyrin, Cross-sectional analysis of composite beams including large initial twist and curvature effects, A.I.A.A. J. 34 (1996) 1913.
[11] O.A. Bauchau, W. Chiang, Dynamic analysis of bearingless tail rotor blades based on nonlinear shell models, J. Aircraft 31 (1994) 1402.
[12] A. Campbell, On vibration galvanometer with unifilar torsional control, Proc. Phys. Soc. 25 (1913) 203.
[13] H. Pealing, On an anomalous variation of the rigidity of phosphor bronze, Philos. Mag. 25 (1913) 418.
[14] J.C. Buckley, The bifilar property of twisted strips, Philos. Mag. 28 (1914) 778.
[15] H. Wagner, Torsion and buckling of open sections, NACA TM 807, 1936.
[16] J.N. Goodier, Elastic torsion in the presence of initial axial stress, Proc. ASME Ann. Conf. Appl. Mech. Division, Purdue University, Lafayette, IN, 1950.
[17] M.A. Biot, Increase of torsional stiffness of a prismatical bar due to axial tension, J. Appl. Phys. 10 (1939) 860.
[18] J.C. Houbolt, G.W. Brooks, Differential equations of motion for combined flapwise bending, chordwise bending and torsion of twisted nonuniform rotor blades, Report 1346, NACA, NACA Technical Note, 1957.

[19] A. Rosen, The effect of initial twist on the torsional rigidity of beams – another point of view, J. Appl. Mech. 47 (1980) 389.
[20] A. Rosen, Theoretical and experimental investigation of the nonlinear torsion and extension of initially twisted bars, J. Appl. Mech. 50 (1983) 321.
[21] M. Borri, T. Merlini, A large displacement formulation for anisotropic beam analysis, Meccanica 21 (1986) 30.
[22] A.D. Stemple, J.-W. Rhim, Y.H. Kim, Vibration analysis of rotating composite beams using finite element model with warping degrees of freedom, Comput. Mech. 16 (1995) 258.
[23] M. Sabuncu, J. Thomas, Vibration characteristics of pretwisted aerofoil cross-section blade packets under rotating conditions, A.I.A.A. J. 30 (1992) 241.
[24] O.G. McGee, Effect of warping-pretwist coupling on the natural vibration of torsional clamped-pinned thin-walled open profile bars, Int. J. Numer. Methods Engng 35 (1992) 325.
[25] K.R.V. Kaza, R.E. Kielb, Effects of warping and pretwist on torsional vibration of rotating beams, J. Appl. Mech. 51 (1984) 913.
[26] D.H. Hodges, A.R. Atilgan, C.E.S. Cesnik, M.V. Fulton, On a simplified strain energy function for geometrically nonlinear behaviour of anisotropic beams, Composites Engng 2 (1992) 513.
[27] D.A. Danielson, D.H. Hodges, Nonlinear beam kinematics by decomposition of the rotation tensor, J. Appl. Mech. 54 (1987) 258.
[28] R.W. Ogden, Non-Linear Elastic Deformation, Section 2.2., Ellis Horwood, Chicester, 1984.
[29] V.L. Berdichevsky, Variational-asymptotic method of shell theory construction, PMM 43 (1979) 664.
[30] V.G. Sutyrin, D.H. Hodges, On asymptotically correct linear laminated plate theory, Int. J. Solids Struct. 33 (1996) 3649.
[31] S.J. Winckler, Hygrothermally curvature stable laminates with tension-torsion coupling, J. Amer. Helicopter Soc. 30 (1985) 56.
[32] E.A. Armanios, A. Makeev, D. Hooke, Finite displacement analysis of laminated composite strips with extension-twist coupling, J. Aerospace Engng 9 (1996) 80.
[33] R. Chandra, A.D. Stemple, I. Chopra, Thin-walled composite beams under bending, torsional, and extensional loads, J. Aircraft, 27 (1990) 619.